ISSN 0023-1584, Kinetics and Catalysis, 2009, Vol. 50, No. 4, pp. 461–473. © Pleiades Publishing, Ltd., 2009.
Original Russian Text © O.V. Skrebkov, S.P. Karkach, A.N. Ivanova, S.S. Kostenko, 2009, published in Kinetika i Kataliz, 2009, Vol. 50, No. 4, pp. 483–496.

Vibrational Nonequilibrium of the HO_2 Radical in the Reaction between Hydrogen and Oxygen at $1000 < T < 1200$ K

O. V. Skrebkov, S. P. Karkach, A. N. Ivanova, and S. S. Kostenko

Institute of Problems of Chemical Physics, Russian Academy of Sciences, Chernogolovka, Moscow oblast, 142432 Russia

e-mail: skreb@inbox.ru

Received March 19, 2008

Abstract—A theoretical model of the chemical and vibrational kinetics of high-temperature hydrogen oxidation is presented. The central feature of this model is that it consistently takes into account the vibrational nonequilibrium of the HO_2 radical as the most important intermediate. The basic distinction between the model and the conventional kinetic schemes is that the former does not consider the reaction $H + O_2 \longrightarrow O + OH$ as an elementary event. Calculated data are presented for $1000 < T < 1200$ K and $0.9 < P < 2.0$ atm, the conditions typical of shock tube experiments. The calculated data show that the nonequilibrium character of the process is the cause of the observed dependence of the "effective rate constant" of the overal reaction $H + O_2 \longrightarrow O + OH$ on experimental conditions. It is demonstrated that this approach is promising from the standpoint of reconciling the predictions of the theoretical model with experimental data obtained by different authors for various compositions and conditions using different methods.

DOI: 10.1134/S0023158409040016

Since the publication of classical works by Semenov and Hinshelwood, the reaction between hydrogen and oxygen has been investigated for more than 70 years. At present, the mechanism of this reaction is considered to be understood best (as compared to, e.g., the mechanism of hydrocarbon oxidation). New experimental and diagnostic methods have been developed to date, extensive experimental data have been accumulated, and the number of possible reactions included in the mechanism of the reaction has become as large as several tens. However, all kinetic calculations performed to interpret experimental data have been based on the assumption that the external and internal degrees of freedom of the molecules and radicals are equilibrated. The relative success in describing experimental data (from the standpoint of practical applications) within the equilibrium approach has been achieved by varying the rate constants of the key processes in wide ranges. The rate constants reported by different authors (see [1]) for the most important chain branching reaction $H + O_2 \longleftrightarrow O + OH$[1] differ markedly, depending on the experimental conditions. About half of the reported values exceed the theoretical upper estimate (for details, see [3, 4]). The theory and experimental data are often reconciled via violation of the relationship between the rate constant of the forward and backward reactions, introduction of nonexistent reactions, and/or use of implausible rate constants (see, e.g., [5, 6]).

Some experimental facts and quantitative comparisons between theoretical and experimental data (for details, see [3, 4]) indicate that it is necessary not only to further refine and detail the kinetic scheme, but also to revise the kinetic conception based on the assumption that the internal (vibrational) degrees of freedom are equilibrated.

According to our earlier work [3], this is particularly true for reactions involving the vibrationally excited radical $HO_2(v)$, which results from the bimolecular recombination reaction $H + O_2 \longrightarrow HO_2(v)$ followed by the redistribution of the $H\cdots O_2$ bond formation energy among the vibrational degrees of freedom (modes) of HO_2, which occurs rapidly at high degrees of vibrational excitation.[2] These reactions are primarily the following key reactions of the conven-

[1] In the oxidation of hydrogen and most hydrocarbons in a typical hydrocarbon flame at atmospheric pressure, about 80% of the oxygen is spent on this reaction [2].

[2] An analysis of the literature [3, 4] and our calculations suggest that the key chain branching reaction $H + O_2 \longrightarrow O + OH$ takes place mainly via an indirect mechanism (the direct mechanism on a quadruplet surface is actually inefficient because of the high activation barrier and small preexponential factor of the rate constant of the corresponding reaction). The indirect mechanism includes the formation of a doublet intermediate complex, specifically, the vibrationally excited radical $HO_2(v)$. The lifetime of this intermediate is comparable with the intercollision time. As a consequence, the effective rate constant of this reaction depends on experimental conditions through vibrational relaxation processes and reactions involving $HO_2(v)$.

tional chain mechanism of hydrogen oxidation: the above reaction $H + O_2 \longleftrightarrow O + OH$ and the chain termination reaction $H + O_2 + M \longleftrightarrow HO_2 + M$. Within the existing (Arrhenius) kinetic conception, these composite reactions (as well as the ones that are less important under the conditions examined) are formally treated as elementary reactions with rate constants depending only on the gas temperature (T).

The inadequacy of this equilibrium kinetic conception, which has become conventional, is illustrated by the fact that it cannot explain the formation of the electronically excited radical OH ($^2\Sigma^+$) at the earliest stages of combustion, even though the OH ($^2\Sigma^+$) $\longrightarrow$ OH+ Q radiation ($Q = 47000$ K, $\lambda \approx 306$ nm) has long been used in experimental practice to determine the ignition delay time. Of the numerous variants discussed in the literature, the only quantitatively acceptable reaction yielding this radical is $H + O_2 + H_2 = OH(^2\Sigma^+) + H_2O$ [7]. We believe that this composite reaction takes place in two steps via the formation of the vibrationally excited radical HO_2: $H + O_2 \longrightarrow HO_2(v)$ and $HO_2(v) + H_2 \longrightarrow OH(^2\Sigma^+) + H_2O$. The overequilibrium excitation of the $HO_2(v)$ radical increases the equilibrium rate constant of the reaction $HO_2 + H_2 \longrightarrow OH(^2\Sigma^+) + H_2O$ by several orders of magnitude.

Here, we report the construction and testing of a theoretical model whose central feature is that it consistently takes into account the vibrational nonequilibrium of the $HO_2(v)$ radical, which is the most important intermediate in chain branching and in the formation of electronically excited species [3]. In this model, the chain branching reaction $H + O_2 \longrightarrow O + OH$ and the chain termination reaction $H + O_2 + M \longleftrightarrow HO_2 + M$ are considered as a single multichannel process that includes the formation of a long-lived intermediate complex, namely, the vibrationally excited radical $HO_2(v)$; intramolecular energy redistribution among the modes of this radical; relaxation of the radical; and its monomolecular decomposition. It is also assumed that this radical can react with other components of the mixture. While the first three processes—energy redistribution among the modes, relaxation, and monomolecular decomposition—can be viewed as the detailing of the Lindemann mechanism for the $H + O_2 \longrightarrow HO_2(v) \longrightarrow O + OH$ reaction that is necessary to explain and predict the dependence of the effective rate constant of this reaction on experimental conditions [3, 4], an adequate description of reactions between $HO_2(v)$ and other components of the mixture would mean a radical revision of the mechanism of chemical reactions in the hydrogen–oxygen system. In this context, ab initio analysis of the processes occurring in the system is of particular significance as an independent source of kinetic information.

KINETIC EQUATIONS

Equations of chemical and vibrational kinetics for the general case of a reacting multicomponent gas mixture within the macroscopic description (for the average energies of vibrational modes (ε_k) and component concentrations (n_i)) were reported for the first time in [8]. Mainly adhering to that work [8] (see also [9]) and using the same notation, we obtain the following expressions for calculating ε_k and n_i at a given gas temperature T and pressure P.

For the molar concentrations of the components per unit mass of the gas mixture (n_i),

$$\rho\frac{dn_i}{dt} = \sum_{r=1}^{L_1}(\nu'_{ir} - \nu_{ir})(R_r - R'_r),$$
$$R_r = k_r\prod_{j=1}^{N}(\rho n_j)^{\nu_{jr}}, \quad R'_r = k'_r\prod_{j=1}^{N}(\rho n_j)^{\nu'_{jr}}, \tag{1}$$
$$i = 1, 2, \ldots, N.$$

Here, ρ is the density of the gas mixture and $R_r(R'_r)$ is the rate of the rth reaction in the forward (backward) direction.

The effect of vibrational relaxation on the kinetics of chemical reactions shows itself as a dependence of the rate constants of these reactions on the average energies of the vibrational modes of the reactants (ε_k) in terms of the corresponding effective vibrational temperatures (T_k):

$$k_r(T, \{T_k\}) = \kappa_r(T, \{T_k\})k_r^0(T). \tag{2}$$

Here, $k_r(k'_r)$ is the rate constant of the rth reaction in the forward (backward) direction; $k_r^0(T)$ is the equilibrium rate constant of the rth reaction; $\kappa_r(T, \{T_k\})$ is the nonequilibrium factor, where $\{T_k\}$ is the set of vibrational temperatures involved in the rth reaction of molecules (reactants), $k = 1, 2, \ldots, b_r$, and b_r is the total number of the vibrational modes of the reactants; and $T_k = \theta_k/\ln[(1 + \varepsilon_k)/\varepsilon_k]$ is the effective vibrational temperature of the kth mode, where θ_k is the characteristic temperature (quantum of the vibrational transition $1 \longrightarrow 0$ in kelvins).

$$\kappa_r(T, \{T_k\}) \cong \exp\left[\frac{E_r}{k}\left(\frac{1}{T} - \frac{\sum_i \beta_{ri}^2}{\sum_i \beta_{ri}^2 T_i}\right)\right],$$
$$E_r = \begin{cases} E_r^a - (\xi_r + 4)kT/2 & \text{for } E_r > 0 \\ 0 & \text{for } E_r \le 0, \end{cases} \tag{3}$$

where E_r is the part of the activation energy of the rth reaction that is associated with the vibrational degrees of freedom (i.e., activation energy minus the equilibrium energy of the relative translational motion ($2kT$) and the equilibrium rotational energy ($\xi_r kT/2$) of the reactant molecules (product molecules at $r = r'$)); ξ_r is the number of rotational degrees of freedom invoiced

in the rth reaction of the molecules; E_r^a is the activation energy of the rth reaction; and β_{ri} are the coefficients of the expansion of the coordinate of the rth reaction in normal modes of the reactants, $\sum_i \beta_{ri}^2 = 1$. In real calculations, we generally postulate a uniform (on the average, statistically) distribution of contributions from the modes of molecules involved in the rth reaction to E_r: $\beta_{r1} = \beta_{r2} = ...$

For the average numbers of the vibrational quanta of the modes (ε_k),

$$\frac{d\varepsilon_k}{dt} = \sum_{q=1}^{L_2} l_{kq} \sum_{i=1}^{N} \gamma_i k_{ji}^{(q)} (Q_q - Q_q') + (\rho n_j)^{-1} \sum_{r=1}^{L_1} (\nu'_{jr} - \nu_{jr})[(\chi_{rk} - \varepsilon_k)(R_r - R_r')], \quad (4)$$

$$Q_q = \prod_m \left[\frac{\varepsilon_m^0 (1 + \varepsilon_m)}{1 + \varepsilon_m^0} \right]^{l_{mq}} \prod_n \left[\frac{\varepsilon_n (1 + \varepsilon_n^n)}{\varepsilon_n^0} \right]^{l_{nq}},$$
$$Q_q' = \prod_m (\varepsilon_m)^{l_{mq}} \prod_n (1 + \varepsilon_n)^{l_{nq}}. \quad (5)$$

Here, $\varepsilon_k^0 = \varepsilon_k(T) = \exp(-\theta_k/T)/[1 - \exp(-\theta_k/T)]$ is the equilibrium value of ε_k (mode k belongs to a molecule of sort j forming in the rth reaction), $\gamma_i = n_i / \sum_i n_i$ is the mole fraction of the ith component, and $k_{ji}^{(q)}$ is the rate constant of the qth channel of vibrational relaxation in the interaction between sort j and i molecules.

The second term on the right-hand sides of the vibrational kinetic equations accounts for the effect of the chemical reactions on vibrational relaxation. Here, χ_{rk} is the average number of vibrational quanta received by the kth mode in one molecule j formation event in the rth reaction (the complete set of χ_{rk} values, where $k = 1, 2, ..., b_r$, characterizes energy distribution among the vibrational modes of the products of the rth reaction):

$$\chi_{rk} = (E_{r'}/\theta_k)\eta_{kr'}, \quad \eta_{kr'} = \beta_{r'k}^2 / \sum_i \beta_{r'i}^2, \quad (6)$$

where $E_{r'}$ is the part of the activation energy of reaction k (backward reaction in which the molecule possessing the r'th mode disappears) that is associated with the vibrational degrees of freedom (defined by Eq. (3)). Within this model (see below), it is natural to assume that the vibrational energy $E_{r'}$ is uniformly distributed between the modes of the products of the rth reaction: $\sum_i \beta_{r'i}^2 = 1, \quad \beta_{r'1} = \beta_{r'2} = ...$

The set of Eqs. (1) and (4) was solved using an implicit difference scheme by the Newton method with automatic control of the time step size, which was set depending on the convergence of the iterations and on the accuracy of approximation. The latter was determined in terms of the second-order divided difference for the solution vector (n_i and ε_k). The input information for the program was the set of chemical reactions and vibrational relaxation channels.

KINETIC SCHEME

In the description of reaction initiation and development in the $H_2 + O_2 + Ar$ system in the temperature range of $1000 < T < 1200$ K and the pressure range of $0.9 < P < 2.0$ atm, we used a kinetic scheme taking into account the chemical reactions involving the species H_2, O_2, H_2O, HO_2, H, O, $OH \equiv OH(^2\Pi)$, H_2O_2, O_3, $O_2^* \equiv O_2(^1\Delta)$, $O^* \equiv O(^1D)$, and $OH^* \equiv OH(^2\Sigma^+)$ and the relaxation channels of the vibrational modes of H_2, O_2, O_2^*, $HO_2(100)$, $HO_2(010)$, and $HO_2(001)$ with characteristic temperatures (θ_k) of 6000, 2250, 2170, 5325, 2059, and 1577 K, respectively [10, 11]. The possible effect of the vibrational nonequilibrium of H_2O_2, H_2O, and O_3 on the reaction initiation and development was ignored because of the low concentrations of these molecules at the process stage examined and because of the high rates of vibrational relaxation. This is less true for the OH radical in the ground electronic state, which forms at a high rate and participates actively in chain propagation via the rapid bimolecular reactions $H_2 + O \longleftrightarrow OH + H$ and $H_2 + OH \longleftrightarrow H_2O + H$. However, according to Eq. (3), these reactions proceed in a practically equilibrium regime ($\kappa \approx 1$) owing to their comparatively low activation energies E_r^a (Table 1).

Chemical Reactions

The mechanism-determining reactions are presented in Table 1. As in our earlier work [3], the values of the equilibrium rate constants $k_r^0(T)$ accepted here are based on NIST reference data [1], results of earlier studies [12–16], our ab initio estimates, and the results of fitting calculated values to experimental data. The basic difference between the kinetic scheme presented in Table 1 and the scheme used in our previous study [3] (and from other similar schemes; see, e.g., [17]) is that the former does not contain the $H + O_2 \longrightarrow O + OH$ reaction as an elementary step. According to the model suggested here (Table 1), the formation of the vibrationally excited radical $HO_2(v)$ is due to the rapid bimolecular recombination reaction (II). The reactivity and further evolution of $HO_2(v)$ are determined by energy redistribution among the vibrational modes, vibrational relaxation, monomolecular decomposition reactions (II') and (III), and numerous reactions involving this radical.

Table 1. Reactions and their equilibrium rate constants, $k_r^0 = A_r(T/298.15)^n \exp(-E_r^a/T)$ ($cm^3\ mol^{-1}\ s^{-1}$), for the $H_2 + O_2 +$ Ar mixture at $1000 < T < 1200$ K and $0.9 < P < 2.0$ atm

r	Reaction	M	A_r	n	E_r^a, K	Note
1	$H + HO_2 \longleftrightarrow H_2 + O_2 + 26.7$[a] (I)		1.46×10^{12}	1.71	−598	[13][b]
2	$H + O_2 \longleftrightarrow HO_2 + 25.5$ (II)		2.0×10^{13}	0.986	–	–
3	$HO_2 \longleftrightarrow O + OH - 33.8$ (III)		3.6×10^{13}	–	33800	[c]
4	$H_2 + OH \longleftrightarrow H_2O + H + 7.5$ (IV)		7.7×10^{11}	1.64	1590	[b]
5	$H_2 + O \longleftrightarrow H + OH - 0.85$ (V)		7.4×10^{12}	0.861	4650	[b]
6	$H_2 + HO_2 \longleftrightarrow HOOH + H - 9.2$ (VI)		2.6×10^{12}	–	10750	[1]
7	$H + HO_2 \longleftrightarrow HO + OH + 17.3$ (VII)		3.8×10^{13}	0.486	103	[1]
8	$O + HO_2 \longleftrightarrow OH + O_2 + 25.7$ (VIII)		1.5×10^{13}	0.33	128	[1]
9	$2OH \longleftrightarrow H_2O + O + 8.5$ (IX)		2.1×10^{10}	2.7	1251	[12]
10	$2HO_2 \longleftrightarrow H_2O_2 + O_2 + 17.5$ (X)		2.8×10^{12}	0.459	158	[1]
11	$OH + HO_2 \longleftrightarrow H_2O + O_2 + 34.1$ (XI)		5.7×10^{13}	−0.322	112	[1]
12	$2H + M \longleftrightarrow H_2 + M + 50.1$ (XII)	M	7.2×10^{15}	−1	−200	[1]
13	$2O + M \longleftrightarrow O_2 + M + 59.0$ (XIII)	M	1.7×10^{14}	−1	–	[1]
14	$H + OH + M \longleftrightarrow H_2O + M + 59.5$ (XIV)	M	9.4×10^{16}	−2	–	[1]
15	$O_2 + O + M \longleftrightarrow O_3 + M + 12.8$ (XV)	M	9.1×10^{13}	1.3	–	[1]
16	$H_2O_2 + M \longleftrightarrow 2OH + M - 5.6$ (XVI)	M	6.1×10^{23}	−5.506	28950	[1]
17	$H+ O + M \longleftrightarrow OH + M + 50.1$ (XVII)	M	1.1×10^{15}	–	–	–
18	$HO_2 + H_2 \longleftrightarrow OH^* + H_2O - 21.9$ (XVIII)		1.2×10^{14}	−0.738	24000	[c]
19	$O^* + H + M \longleftrightarrow OH^* + M + 27.5$ (XIX)		7.0×10^{15}	−1	–	[c]
20	$O + H + M \longleftrightarrow OH^* + M + 4.5$ (XX)	H_2	5.6×10^{11}	0.18	4040	[c]
		O_2, Ar	5.0×10^{15}	−1.0	12000	
		OH	2.0×10^{15}	−1.0	–	
21	$OH^* + M \longleftrightarrow OH + M + 47.0$ (XXI)	M	1.3×10^{11}	0.5	–	[14, 15][c]
22	$OH^* + O_2 \longleftrightarrow O_3 + H + 8.5$ (XXII)		4.0×10^{13}	0.5	–	[14, 15][c]
23	$OH^* + H_2O \longleftrightarrow H_2O_2 + H + 12.7$ (XXIII)		7.5×10^{12}	–	276	[14, 15][c]
24	$OH^* + H_2 \longleftrightarrow H_2O + H + 54.3$ (XXIV)		8.5×10^{13}	0.5	–	[14, 15][c]
25	$OH^* + O_2 \longleftrightarrow HO_2 + O + 21.0$ (XXV)		2.0×10^{13}	0.5	–	[14, 15][c]
26	$OH^* \longleftrightarrow OH + h\nu$, $h\nu = 47.0$ (XXVI)		1.4×10^{6}	–	–	[16]
27	$H + HO_2 \longleftrightarrow H_2O + O^* + 3.3$ (XXVII)		4.8×10^{13}	–	892	[1][d]
28	$O^* + H_2 \longleftrightarrow OH + H + 25.3$ (XXVIII)		9.0×10^{13}	–	−14.1	[1]
29	$O^* + M \longleftrightarrow O + M + 23.0$ (XXIX)	M	2.0×10^{11}	–	–	[1]
30	$H + HO_2 \longleftrightarrow H_2 + O_2^* + 15.4$ (XXX)		6.5×10^{11}	1.67	3160	[b]
31	$O_2 + M \longleftrightarrow O_2^* + M - 11.3$ (XXXI)	H_2	1.0×10^{6}	0.03	11380	[1]
		O_2	6.6×10^{5}	0.03	11380	
		Ar	2.0×10^{5}	0.03	11380	
32	$O_2^* + H \longleftrightarrow OH + O + 3.8$ (XXXII)		7.0×10^{13}	0.779	7000	[b, c]
33	$O^* + H_2 \longleftrightarrow OH^* + H - 25.4$ (XXXIII)		8.0×10^{13}	–	25200	–
34	$OH + O + H_2 \longleftrightarrow OH^* + H_2O + 12.1$ (XXXIV)		1.0×10^{18}	–	15000	–
35	$2OH + H \longleftrightarrow OH^* + H_2O + 13.1$ (XXXV)		1.0×10^{18}	–	15000	–

Note: [a] The heats of the reactions are in 10^3 K.
[b] CTST estimate.
[c] Fitting to experimental data.
[d] LST [3] and DRC [3].

Intramolecular Redistribution of Vibrational Energy among the Modes of HO_2

Since the lifetime of the HO_2 intermediate is comparable with the characteristic intercollision time [3, 18], it is natural to believe that, between collisions, a significant role is played by intramolecular energy exchange between modes. It is also pertinent to assume that this process becomes still more important as the degree of vibrational excitation increases (as a consequence of the anharmonicity of molecular vibrations, the appearance of resonances, and the strengthening of the vibrational–rotational (VR) interaction) from weak intermode interaction at low energies (or the absence of this interaction[3]) to complete "mode mixing" and uniform energy distribution among the modes at high energies, when the oscillators (modes) can be treated as classical oscillators with equal heat capacities. In the case of the HO_2 radical, which results from the bimolecular recombination reaction $H + O_2 \longrightarrow HO_2$, the energy of the $H\cdots O_2$ bond ($D \approx 25\,500$ K) is redistributed almost instantaneously (in comparison with the characteristic intercollision time) among the modes down to a value of $E_0 \approx D/3$ per mode. At these energies ($E_0 \approx 8500$ K), the intramolecular intermode energy exchange takes a time on the order of the vibration period ($\sim 10^{-13}$–10^{-14} s). In progress of relaxation, as the degree of vibrational excitation becomes smaller, the rate of this process decreases.

As for the dependence of the intramolecular vibrational exchange rate on the excitation energy, this aspect of dynamics was not studied for the HO_2 radical. The calculations (both classical and quantum) carried out for other triatomic molecules, such as H_2O (see [20, 21] and references therein), as well as the calculations of the dynamics of the dissociation and recombination of HO_2 via the Lindemann mechanism [22–24], indicate the admissibility of the following assumptions made here: (1) on the average (statistically), the energy exchange between modes of HO_2 is directed toward the leveling of the energies of the vibrational modes, $E_k = \theta_k\varepsilon_k$; (2) the rate constant of intramolecular exchange is energy-dependent, decreasing as the degree of vibrational excitation decreases.

Formulating the kinetic problem, we will postulate that the rate constant of intramolecular energy exchange between modes of HO_2 in the absence of collisions depends on the degree of vibrational excitation:

$$(q = 1)\ HO_2(3E\,0\,0) \longleftrightarrow HO_2(E\,E\,E),$$

$$k_V^{(1)} = A_0 \exp\left[-\delta_1\left(1 - \frac{\varepsilon_2}{\delta_2}\right)^2\right].$$

Here, we set $\delta_1 = 14.0$, $\delta_2 \approx E_0/\theta_2 = 1.65$, and $A_0 = 8 \times 10^{13}$ s^{-1} (as the result of fitting to experimental data). The net rate of process (1) in the forward direction, which is a term in the vibrational kinetic equations (4), is expressed as

$$Q_1 - Q_1' = \frac{(E/\theta_4)(1+\varepsilon_4)}{1+E/\theta_4}\frac{\varepsilon_5(1+E/\theta_5)}{E/\theta_5} \times \frac{\varepsilon_6(1+E/\theta_6)}{E/\theta_6} - \varepsilon_4\frac{1+\varepsilon_5}{E/\theta_5}\frac{1+\varepsilon_6}{E/\theta_6}.$$

That is, it has the form of Eq. (5), but with $\varepsilon_k^0 = E/\theta_k$, where $k = 4$, 5, and 6 are the numbers of modes of HO_2. Here, $E \equiv E(t) = (\varepsilon_4\theta_4 + \varepsilon_5\theta_5 + \varepsilon_6\theta_6)/3$ is the current nonequilibrium value of energy per mode of HO_2 for the uniform energy distribution. The effect of process (I) on the relaxation of the vibrationally excited radical HO_2, directed toward the leveling of the vibrational mode energies, leads to an increase in the number of vibrational quanta in the high-frequency mode ($k = 4$) through a decrease in the number of vibrational quanta in the low-frequency modes ($k = 5$ and 6) (for details, see [25]). The main result of intramolecular energy redistribution into uniform distribution is that the final state is nonequilibrium, quasi-steady-state, with an overpopulated high-frequency mode and an underpopulated low-frequency mode relative to the equilibrium state. In other words, the rapid leveling of the energies of the modes of HO_2 (as compared to the other processes) at comparatively high excitation energies is a kind of "disequilibrium generator."

Collisional Intermolecular Vibrational Energy Exchange

The channels of vibrational–translational (VT) exchange and the corresponding characteristic times $\tau_q^{(M)}$ are presented in Table 2. The VT relaxation data for diatomic molecules (processes with $q = 2$–4 in Table 2) are based on the results reported in [26–28] and seem to be the most reliable.

As for the kinetics of the VT relaxation of the vibrational modes of HO_2 on different species M (here, H_2, O_2, Ar, and H_2O), note first of all that this aspect of the behavior of the HO_2 radical has been poorly investigated both experimentally and theoretically. This is also true for the quantitative kinetic aspect of VV' exchange in the mixture as a whole. Table 3 present the most significant VV' relaxation channels and their rate constants as $k_{ji}^{(q)} = a_{ji}^{(q)}\exp(-b_{ji}^{(q)}T^{-1/3})$. We believe that this representation is adequate to the narrow temperature range examined. The relaxation times ($\tau_5^{(M)}$) and rate constants $k_{ji}^{(q)}$ ($q = 6$–14) listed in Tables 2 and 3

[3] This assumption is known as local mode approximation (see [19] and references therein).

Table 2. VT relaxation processes and their characteristic times, $\tau_q^{(M)} = a_q^{(M)} \exp(b_q^{(M)} T^{-1/3})$ (s atm), for the $H_2 + O_2 + H_2O + Ar$ mixture at $1000 < T < 1200$ K

q[a]	Vibrational relaxation channel $X_j(1) + M \leftrightarrow X_j(0) + M$	M	$a_q^{(M)}$	$b_q^{(M)}$	$\tau_q^{(M)}\big\|_{1100\ K}$	Note
2	$H_2(1) + M \leftrightarrow H_2(0) + M$	H_2, H_2O	1.20×10^{-10}	100	1.9×10^{-6}	[16–18][b]
		O_2	2.40×10^{-10}	101	4.3×10^{-6}	
		Ar	9.20×10^{-10}	104	2.2×10^{-5}	
3	$O_2(1) + M \leftrightarrow O_2(0) + M$	H_2, H_2O	1.89×10^{-9}	49.5	2.3×10^{-7}	[16–18][b]
		O_2	1.00×10^{-10}	138	6.4×10^{-5}	
		Ar	5.00×10^{-11}	173	9.5×10^{-4}	
4	$O_2^*(1) + M \leftrightarrow O_2^*(0) + M$	H_2, H_2O	2.14×10^{-9}	48.0	2.2×10^{-7}	[16–18][b]
		O_2	1.10×10^{-10}	134	4.8×10^{-5}	
		Ar	5.60×10^{-11}	169	7.2×10^{-4}	
5	$HO_2(001) + M \leftrightarrow HO_2(000) + M$	H_2	2.53×10^{-9}	11.85	8.0×10^{-9}	b, c
		O_2	8.62×10^{-8}	11.60	2.7×10^{-7}	b, c, d
		H_2O	6.01×10^{-10}	12.37	2.0×10^{-9}	b, c, d
		Ar	2.53×10^{-7}	11.85	8.0×10^{-7}	b, d

[a] For $q = 2$–5, $k_{jM}^{(q)} = P(1 + \varepsilon_k^0)/\tau_k^{(M)}$, $\sum_i \gamma_i k_{ji}^{(q)} \equiv \sum_M \gamma_M k_{jM}^{(q)}$. For designations, see Eq. (4).

[b] Fitting to experimental data.

[c] SSHM estimate.

[d] SSH estimate.

are obtained by fitting calculated t_{50} and t^* data to experimental data [12, 29, 30] (see below). The initial values in $\tau_5^{(M)}$ and $k_{ji}^{(q)}$ fitting were estimates obtained by us using the Schwartz–Slavsky–Herzfeld (SSH) theory [31] (see also [32]), as well as the Schwartz–Slavsky–Herzfeld–Moore (SSHM) variant of this theory, which takes into account VR energy transfer in the simplest way [33] (see also [34, 35]). The basic formulas used in the SSH and SSHM estimation procedures are presented in the Appendix.

The SSH and SSHM calculations of the characteristic times of the VT relaxation of the vibrational modes of HO_2 are based on the assumption that these times are independent; that is, the collision-induced perturbations are neglected. For the HO_2 radical (which is a nonlinear molecule executing angular bending vibrations), these perturbations are likely not small. For maximum simplification of the collision-induced intermode interaction problem, which is far from being solved, we will represent the molecule as a single set of coupled oscillators exchanging energy with translational and/or rotational degrees of freedom through the most rapidly relaxing mode.[4] In the case considered, this is one of the low-frequency modes of HO_2.

RESULTS AND DISCUSSION

The calculated data presented in this section illustrate the efficiency of the above approach and its potential for elucidating the physical essence of high-temperature hydrogen oxidation (as a process essentially nonequilibrium with respect to vibrational degrees of freedom) and for quantitative interpretation of experimental data.

In our calculations, we used a coordinate system associated with the gas stream behind the wave front (the gas mixture is at rest, $P = \text{const}$, $T = \text{const}$, and $t = 0$ is the instant when the shock front passes).

[4] A discussion of this approach applied to the CO_2 and relevant bibliography can be found in a review by Nikitin and Osipov [36].

Table 3. VV' exchange channels and their rate constants, $k_{ji}^{(q)} = a_{ji}^{(q)} \exp(-b_{ji}^{(q)} T^{-1/3})$ (s^{-1}), for the $H_2 + O_2 + O_2^* + HO_2$ mixture at $1000 < T < 1200$ K

q	Channel of vibrational exchange between oscillators, A(1) + B(0) ⟷ A(0) + B(1)	$\frac{\theta_B}{\theta_A}$	$a_{AB}^{(q)}$	$b_{AB}^{(q)}$	$k_{ji}^{(q)}\big\|_{1100\ K}$	Note
6	$H_2(1) + HO_2(000) \longleftrightarrow H_2(0) + HO_2(100)$	0.89	6.82×10^5	−0.12	7.0×10^5	a, b
7	$H_2(1) + O_2(0) \longleftrightarrow H_2(0) + O_2(1)$	0.37	4.52×10^6	63.56	9.7×10^3	a, b, c
8	$H_2(1) + O_2^*(0) \longleftrightarrow H_2(0) + O_2^*(1)$	0.36	5.31×10^6	67.85	7.6×10^3	a, b, c
9	$HO_2(100) + O_2(0) \longleftrightarrow HO_2(000) + O_2(1)$	0.42	2.65×10^7	81.36	1.1×10^4	a, b
10	$HO_2(100) + O_2^*(0) \longleftrightarrow HO_2(000) + O_2^*(1)$	0.41	2.79×10^6	60.29	8.3×10^3	a, b
11	$O_2(1) + HO_2(000) \longleftrightarrow O_2(0) + HO_2(010)$	0.92	8.84×10^4	−9.35	2.2×10^5	a, b
12	$O_2(1) + O_2^*(0) \longleftrightarrow O_2(0) + O_2^*(1)$	0.97	1.97×10^5	−11.56	6.0×10^5	a, b
13	$O_2^*(1) + HO_2(000) \longleftrightarrow O_2^*(0) + HO_2(010)$	0.95	7.00×10^4	−12.77	2.4×10^5	a, b
14	$HO_2(010) + HO_2(000) \longleftrightarrow HO_2(000) + HO_2(001)$	0.77	2.30×10^5	0	2.3×10^5	a, b

[a] Fitting to experimental data.
[b] SSHM estimate.
[c] SSH estimate.

Comparison between Calculated and Experimental Data

Direct kinetic investigation of processes under real conditions of nature or technology (e.g., combustion and detonation) is complicated by side factors, namely, diffusion, heat release, heat transfer, and convection, which occur simultaneously with the main chemical process and, in some cases, can play the determining role. Because of this, a large number of parameters are introduced into theoretical models (in addition to kinetic characteristics). In many cases, these parameters either are unknown or have a high degree of uncertainty. This markedly complicates the quantitative interpretation of experimental data, introducing uncertainty into model kinetic schemes.[5] In this study, the experimental data to be compared with kinetic (isothermal) calculations are shock-tube data for $H_2 + O_2$ mixtures heavily diluted with Ar [12, 29, 30]. The results of these experiments can be compared directly with the results of isothermal kinetic calculations because the authors took special care to minimize the effect of such a "nonkinetic" factor as the self-heating of the mixture, when gas dynamic and thermal phenomena come to the foreground.

In Table 4, the kinetic data calculated using the above model within one kinetic scheme (Tables 1–3) are compared with the corresponding experimental data [12, 30]. The experiments [12, 30] were carried out by the shock-wave method (P and T are the pressure and temperature behind the front of the reflected [12] or incident [30] wave). On the whole, the calculated data are in qualitative and quantitative agreement with the experimental data (in the worst case (entry 4), the discrepancy is 24%). Note that, in the fitting of the calculated t^* and t_{50} data to experimental data, the main point was variation and fitting of the unknown kinetic constants $\tau_5^{(M)}$ and $k_{ji}^{(q)}$ ($q = 1, 6, 9, 10, 11, 13, 14$), which characterize the vibrational–translational, intramolecular, and vibrational–vibrational exchange processes involving the vibrational modes of HO_2. In future studies, in which the composition and condition (temperature and pressure) ranges will be widened, we are going to refine the kinetic constants k_r^0, $\tau_q^{(M)}$, and $k_{ji}^{(q)}$ (Tables 1–3) to take into account the changes in the roles of the components and reactions considered here and the new processes included in the kinetic scheme.

Dependence of the Effective Rate Constant of Chain Branching on Reaction Conditions and the Vibrationally Nonequilibrium Character of the Process

As was noted above, the mechanism postulated here does not include the elementary reaction $H + O_2 \longrightarrow O + OH$, whose activation energy is $6790 \le E^a \le 11430$ K, according to carious experimental esti-

[5] In this context, it is pertinent to quote the following statement from an article by Basevich et al. [37]: "The kinetic mechanism of reactions determines, to a considerable extent, the physicochemical characteristics of combustion, including the combustion rate and the product composition. This makes it possible to use these characteristics in the approbation of various kinetic schemes. However, it should be taken into account that obtaining a satisfactory description of combustion characteristics is a necessary, but not sufficient, condition."

Table 4. Experimentally measured [12[a], 30[b]] and calculated (within one kinetic scheme[c]) values of t_{50}^{d} and t^{*e}

Entry	T, K	P, atm	Experiment		Calculation	
			t^*, μs [30]	t_{50}, μs [12]	t^*, μs	t_{50}, μs
1	1050	1.900	945–1120	–	1102	–
2	1225	1.500	600	–	603	–
3	1052	2.200	–	618	–	525
4	1074	0.935	–	1005	–	1241
5	1086	0.940	–	985	–	1130
6	1102	1.200	–	836	–	911
7	1115	2.248	–	393	–	404

[a] Experimental conditions: reflected shock wave, rich mixture (4% H_2 + 1% O_2 + 95% Ar), measurement of absorption by OH.

[b] Experimental conditions: incident shock wave, stoichiometric mixture (0.93% H_2 + 0.46% O_2 + 98.61% Ar), measurement of emission from OH*.

[c] See Tables 1–3.

[d] Time interval between the passage of the shock front and the moment at which light absorption by the OH radical reaches its half-maximum (in calculations, the moment at which the OH concentration reaches its half-maximum).

[e] Time interval between the passage of the shock front and the moment of maximum emission at ~306 nm (in calculations, the maximum OH* concentration moment).

mates [1]. As will be demonstrated below, the rate of chain branching is determined by the rate of the monomolecular decomposition of the vibrationally excited radical HO_2 (Table 1, reaction (III)). The rate constant of the overal reaction $H + O_2 \longrightarrow O + OH$ will be derived from the calculations as $k_{eff} = R_3/[H][O_2]$. Its dependence on experimental conditions is illustrated by Fig. 1, which shows the time plots

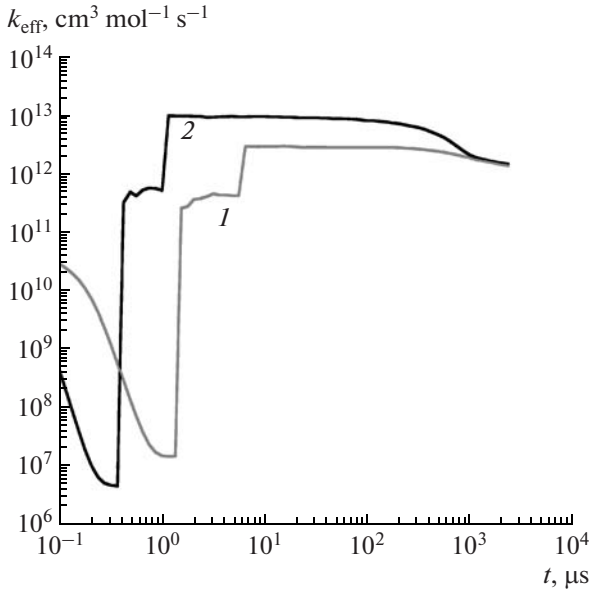

Fig. 1. Time dependences of k_{eff} for two calculation variants: (*1*) $T = 1050$ K, $P = 1.9$ atm, stoichiometric mixture, measurement of emission from OH* (entry 1 in Table 4); (*2*) $T = 1052$ K, $P = 2.2$ atm, rich mixture, measurement of absorption by OH (entry 3 in Table 4).

of the k_{eff} data calculated for experiments 1 [30] and 3 [12] (Table 4), performed at nearly the same temperature of $T \cong 1050$ K.

The clearly defined pressure and time dependences of the effective rate constant of the key composite reaction determining the rate of the overall process are due to the nonequilibrium character of this reaction and to the changes in the roles of various elementary reactions and vibrational relaxation channels at various stages of the process. The essentially nonequilibrium character of hydrogen oxidation with respect to vibrational degrees of freedom is illustrated by Figs. 2 and 3, which plot the typical time dependences of the vibrational temperature T_k and nonequilibrium factor $\kappa_r(T,\{T_k\})$, respectively, for the most important reactions under the conditions examined.

The following three stages of vibrational relaxation can be distinguished in Fig. 2:

(1) At $t < 10$ μs, the initial H_2 and O_2 molecules undergo vibrational excitation from the initial (near-room) temperature T_0 to the equilibrium gas temperature T behind the front of the shock wave. Negligible amounts of HO_2 and O_2^* (see Figs. 4 and/or 5) with equilibrium temperatures equal to the gas temperature (Fig. 3, curves *2*, *5*, *6*, *4*) result from the initiation reaction (I') and shock-induced (collision-induced) electronic excitation (process (XXXI)). The only source of the overequilibrium vibrational excitation of HO_2 is the activationless bimolecular recombination reaction (II) (which is the main excitation source throughout the process). The variation of the rate of this reaction is determined by the variation of the quantity of H atoms. The first quasi-steady state (plateau in Fig. 3) arises from the competition between "chemical pumping" (due to the recombination of H atoms

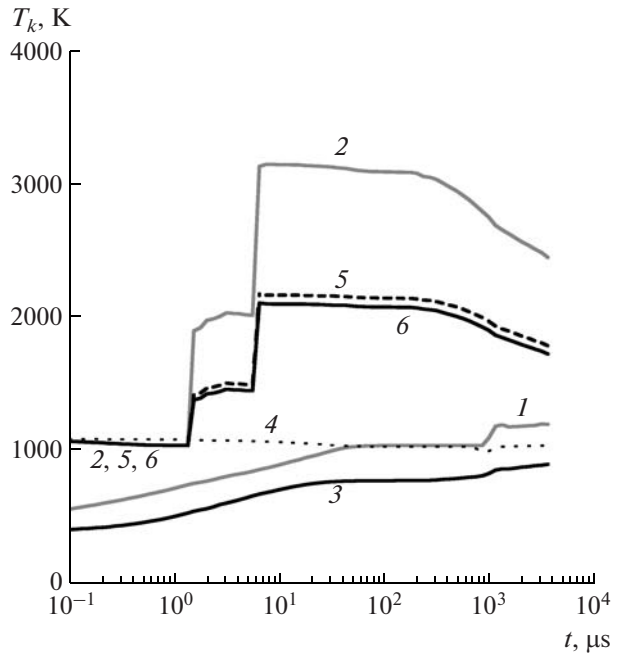

Fig. 2. Typical time dependences of the vibrational temperature T_k under the conditions examined. The curves are numbered in the order of decreasing characteristic temperatures of vibrational modes (θ_k): (*1*) H_2, (*2*) $HO_2(100)$, (*3*) O_2, (*4*) O_2^*, (*5*) $HO_2(010)$, and (*6*) $HO_2(001)$. This figure and the figures presented below illustrate calculation variant 1 in Table 4.

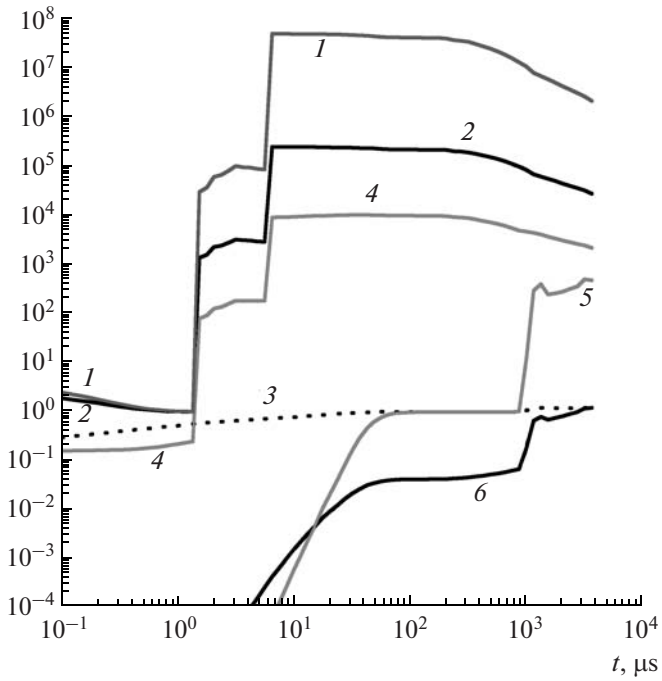

Fig. 3. Typical time dependences of the nonequilibrium factor $\kappa_r(T,\{T_k\}) = k_r(T,\{T_k\})/k_r^0(T)$ under the conditions examined for various reactions (Table 1): (*1*) reaction (III), (*2*) reverse reaction (II'), (*3*) reaction (V), (*4*) reaction (XVIII), (*5*) reverse reaction (XII'), and (*6*) reverse reaction (I').

resulting from the initiation reaction (I') with O_2 molecules) and the vibrational deactivation of HO_2. The rapid buildup of the vibrational excitation of HO_2 is the chemical pumping resulting from the rapid formation of H atoms via reactions (III)–(V) and their recombination with initial O_2 molecules.

(2) The time interval $10 \le t < 1000$ μs corresponds to the quasi-steady-state stage at which the vibrationally excited radical $HO_2(v)$ forms and accumulates as a result of the bimolecular recombination reaction (II), intramolecular energy redistribution until uniform distribution ($HO_2(3E\,0\,0) \leftrightarrow HO_2(E\,E\,E)$), and vibrational relaxation. The second prolonged quasi-steady state arises from the competition of chemical pumping with vibrational deactivation and with the disappearance of vibrationally excited HO_2 in endothermic reactions.

(3) At $t \ge 1000$ μs, the vibrational excitation of $HO_2(v)$ decreases because of relaxation and the disappearance of high-energy molecules via endothermic reactions, such as reaction (III), which is the main reaction ensuring chain branching. This is accompanied by the growth of the vibrational excitation of H_2 and O_2 via vibrational–vibrational exchange and via the formation of these molecules as secondary species in exothermic reactions (XI) and (XXX) (Table 1).

The time dependences of the nonequilibrium factor $\kappa_r(T,\{T_k\})$ for reactions (I'), (II'), (III), (V), (XII'), and (XVIII) at the vibrational temperatures T_k examined in Fig. 2 are shown in Fig. 3. Clearly, taking into account the vibrational nonequilibrium points out very important effects taking place throughout the process. The rate constants of reactions depend on the vibrational temperatures of the reactants, and this dependence is characterized by a factor as large as several orders of magnitude. This is particularly true for reactions involving the HO_2 radical. For example, within the model considered, the nonequilibrium factor for reaction (XVIII), which is responsible for the formation of the electronically excited radical OH* throughout the induction period, is $\kappa_{18} \approx 10^4$, and the nonequilibrium factor for the key reaction (III), which mainly determines the chain branching rate, is $\kappa_3 \sim 10^8$. This large deviation of κ_r from unity means that the reaction between hydrogen and oxygen is an essentially nonequilibrium reaction and that the vibrational nonequilibrium of the HO_2 radical is an intrinsic feature of hydrogen oxidation.

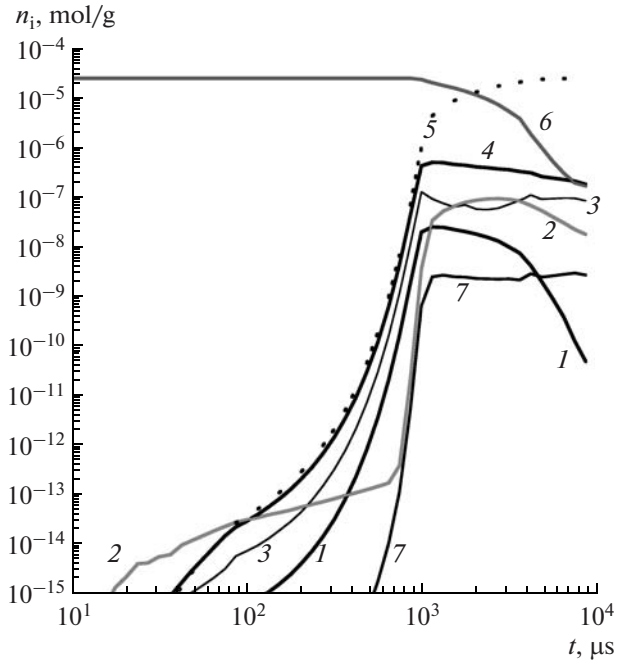

Fig. 4. Time dependences of the concentrations (n_i) of (*1*) HO_2, (*2*) O_2^*, (*3*) OH, (*4*) H, (*5*) H_2O, (*6*) H_2, and (*7*) H_2O_2 in the reacting $H_2 + O_2 + Ar$ mixture behind the shock wave.

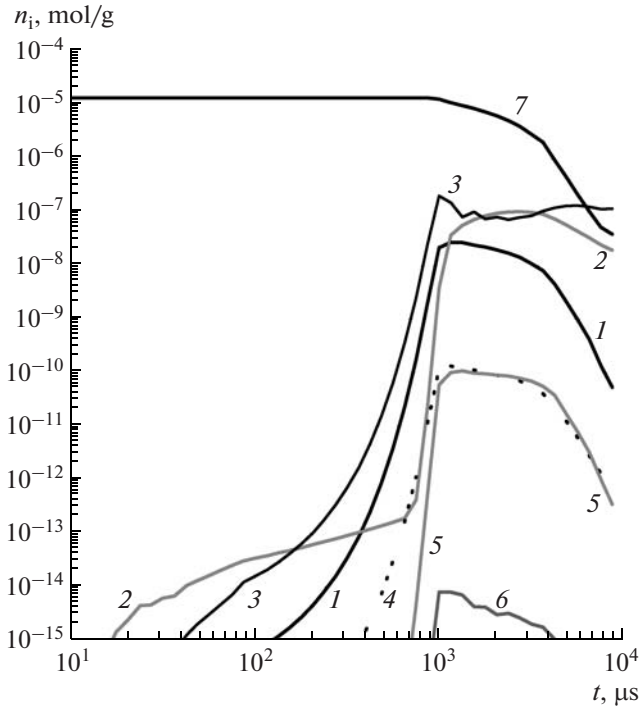

Fig. 5. Time dependences of the concentrations (n_i) of (*1*) HO_2, (*2*) O_2^*, (*3*) O, (*4*) O_3, (*5*) O*, (*6*) OH*, and (*7*) O_2 in the reacting $H_2 + O_2 + Ar$ mixture behind the shock wave.

Kinetics of Chemical Reactions at Various Stages of the Process

Figures 4 and 5 illustrate the typical behavior of component concentrations in the reacting $H_2 + O_2 + Ar$ mixture behind a shock wave under the conditions examined.

First of all, note that considerable amounts of singlet dioxygen O_2^* appear at the earliest stages of the reaction (Figs. 4, 5). During the reaction, the O_2^* concentration reaches a level indicating that singlet dioxygen is among the major intermediates along with HO_2, H, O, and OH.[6] Note that this conclusion was not influenced qualitatively by variation of the rate constant of O_2^* quenching (reaction (XXXI')) by two orders of magnitude. This variation was performed under the condition that the relationship $k_{31}^0/k_{31'}^0 = K_{31}$ is true (K_{31} is the equilibrium constant of reaction (XXXI)).

As estimated from the behavior of the initial components H_2 and O_2, the induction period of the reaction in this particular variant of calculation (stoichiometric mixture, $T = 1050$ K, $P = 1.9$ atm) continues up to $t \approx 800$ μs. Depending strongly on reaction conditions (composition, temperature, and pressure), the induction period end time and the onset and end times of the intensive stage of the reaction in all cases are equal to the times at which the HO_2 concentration is near its maximum.

A very significant characteristic of a reaction is its rate, which determines its role (contribution) at a particular stage of the complex chemical reaction in the multicomponent reacting mixture. Figure 6 plots the rates ($w_r = R_r/\rho$, $mol^{-1}\ s^{-1}$) of reactions (I') and (XXXI), which are the rate-determining reactions at the active site generation stage, the initial stage of the chain process. At the intensive reaction stage, the most rapid reactions are the monomolecular decomposition of the vibrationally excited radical $HO_2(v)$ (reaction (III)), which is the key chain branching reaction under the conditions examined, and by reaction (IV), which is the main reaction responsible for chain propagation. Figure 6 also plots the rates of fast reactions (I), (VII), and (XXX), which involve the HO_2 radical. The high rates of these reactions are due to the fairly high reactant concentrations at this stage of the process (Figs. 4, 5). Reactions (I) and (XXX) are responsible for the formation of vibrationally excited O_2 and O_2^* at this stage, and reaction (VII) should be considered as one of the most significant OH formation channels, next in importance to reaction (III).

[6] In practical kinetic calculations, singlet dioxygen and its reactions are usually ignored unless this component is artificially introduced into the calculation in order to simulate the effect of discharge or radiation (see, e.g., [5, 6] and references therein).

Note that it is the fast reactions (IV), (I), and (XXX), which accompany the equally fast reactions (III) and (VII) and release energy largely as the energy of the translational and rotational motion of molecules (see relationships (6) and (3) for $E_{r'}$), that are responsible for the explosive character of the self-heating of the reaction mixture in hydrogen combustion and detonation.

CONCLUSIONS

A theoretical model has been constructed and approbated, whose central feature is that it consistently takes into account the vibrational nonequilibrium of the HO_2 radical as the key intermediate in chain branching and in the formation of electronically excited species. Our calculations have illustrated the potential of this approach from the standpoint of establishing the physically adequate mechanism of hydrogen ignition and combustion in order to fit the theoretical model to experimental data obtained by different authors for various compositions and conditions using different methods.

According to the calculations within this model, the $H_2 + O_2$ reaction proceeds so that the vibrational degrees of freedom are not equilibrated. The actual rate constants may differ from their equilibrium values by several orders of magnitude. Under the conditions examined, this reaction is essentially nonequilibrium and the vibrational nonequilibrium of the HO_2 radical is an intrinsic feature of hydrogen oxidation. The nonequilibrium character of the process with respect to vibrational degrees of freedom is responsible for the observed dependence of the effective rate constant of the overal reaction $H + O_2 \longrightarrow O + OH$ on experimental conditions.

Owing to the participation of the HO_2 radical in the oxygen regeneration reaction ($H + HO_2 \longrightarrow H_2 + O_2(^1\Delta)$), the $O_2(^1\Delta)$ concentration reaches a fairly high level making the singlet dioxygen molecule as important as the intermediate species HO_2, H, O, and OH.

We think that further improvements to the model taking into account the essentially nonequilibrium character of high-temperature hydrogen oxidation should be made by taking into consideration the reactions of $HO_2(v)$ with other mixture components revealed by preliminary ab initio investigation (primarily the initial reactants H_2 and O_2).

APPENDIX

Since the harmonic oscillator model is used here, the probability of the vibrational exchange process

$$\{v_m; v_n\} \xrightarrow{P_{ji}^{(q)}(m;n)} \{v_m - l_{mq}; v_n + l_{nq}\}, \qquad (A.1)$$

in which, upon a collision between a sort i molecule and a sort j molecule, as a result of the qth process the vibrational quantum numbers v_m in modes m decrease by l_{mq} and the vibrational quantum numbers v_n in modes n increase by l_{nq}, is uniquely determined by the probability of the corresponding transition between the lowest states, $P_{ji}\begin{Bmatrix} l_{mq}, 0 \\ 0, l_{nq} \end{Bmatrix}$.[7] Practical use of kinetic quantities of this type, which characterize a given vibrational exchange process as taking place between modes each treated as a single whole, implies replacement of expression (A.1) with

$$\{l_{mq}; 0\} \xrightarrow{P_{ji}^{(q)}(m;n)} \{0; l_{nq}\}. \qquad (A.2)$$

According to SSH theory [31] (see also [32]), the probability of the qth complex transition of vibrational energy from modes m to modes n per collision in the interaction between sort j and i molecules is calculated as

$$P_{ji}^{(q)}(m;n) \equiv P_{ji}\begin{Bmatrix} l_{mq}, 0 \\ 0, l_{nq} \end{Bmatrix} = \zeta \prod_m V_{l_{mq},0}^2 \prod_n V_{l_{nq},0}^2 \times \Phi[\xi_0^{(m)}(1 - \omega_n/\omega_m)]. \qquad (A.3)$$

Here, ζ is the orientation factor (taken to be 0.1), $V_{l_{sq},0}$ is the matrix element of the $0 \longrightarrow l_{sq}$ transition of the sort s harmonic oscillator (mode) involved in the qth

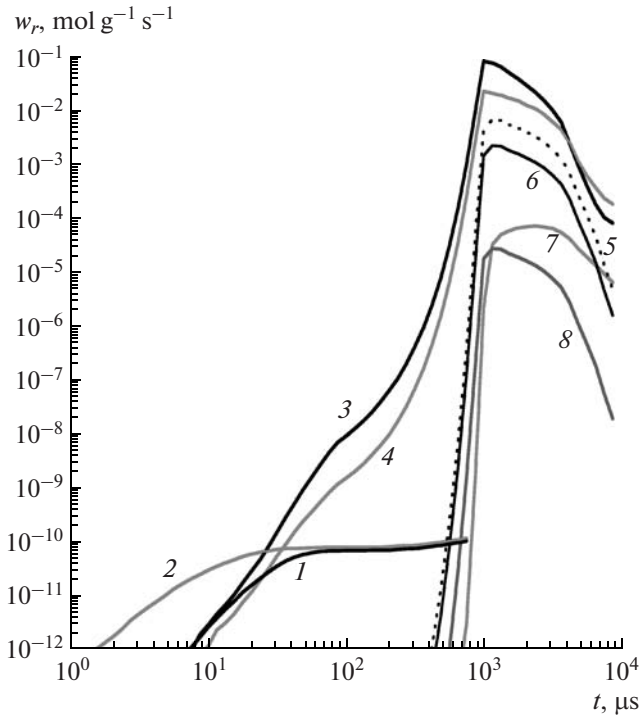

Fig. 6. Time dependences of reaction rates (w_r) at the chain process development and intensive reaction stages behind the shock wave (Table 1): (*1*) (I'), (*2*) (XXXI), (*3*) (III), (*4*) (IV), (*5*) (VII), (*6*) (I), (*7*) (XXXII), and (*8*) (XXX).

[7] In the simplest case of one-quantum VT exchange, this correlation is defined by the expression $P_{n,n-1} = nP_{10}$.

process, ω_s is the vibration frequency of the sort s oscillator, $\xi_0^{(m)} = \tau_*\omega_m$ is the adiabaticity parameter (collision-averaged Massey parameter), τ_* is the characteristic interaction time, and $\Phi(x)$ is the adiabaticity factor accounting for the change in translational energy in VT exchange.

The function

$$\Phi(x) = x^2\int_0^\infty e^{-z}\operatorname{cosech}h^2(x/\sqrt{z})dz$$
$$\cong \begin{cases} 8\sqrt{\pi/3}x^{7/3}\exp(-3x^{2/3}), & x \gg 1 \\ \frac{1}{2}\left[3-\exp\left(-\frac{2}{3}x\right)\right]\exp\left(-\frac{2}{3}x\right), & 0 \le x \le 20, \end{cases} \quad (A.4)$$

the adiabaticity parameter

$$\xi_0^{(m)} = \pi\beta\alpha^{-1}(D/kT)^{-1/2}(M/\mu)^{-1/2}, \quad (A.5)$$

and the matrix elements

$$V = \frac{1}{\sqrt{2}}(\beta/\alpha) \quad (A.6)$$

(with only one-quantum transitions taken into account) are derived from relationships well-known in vibrational relaxation theory (see, e.g., [38–42] and references therein). Here, M is the reduced mass of the colliding species, μ is the reduced mass of the oscillator, α^{-1} is the characteristic radius of action of the intermolecular potential, and D and β are parameters of the intramolecular potential (Morse potential).

When formulas (A.3)–(A.6) were applied to the HO_2 molecule, the latter was treated as a set of the following harmonic oscillators: vibration of the H···O bond ($HO_2(100)$) with a reduced mass of 1.0693 and a frequency of 3698 cm^{-1}, bending vibration relative to the equilibrium ∠HOO angle of 104.3° ($HO_2(010)$) with a reduced mass of 1.1311 and a frequency of 1430 cm^{-1}, and vibration of the O···O bond ($HO_2(001)$) with a reduced mass of 13.0737 and a frequency of 1120 cm^{-1}.

For the VT exchange and strongly nonresonant VV' exchange processes involving the $HO_2(100)$ and $HO_2(010)$ oscillators (which are asymmetric because of the presence of a hydrogen atom), the rotational velocity can be higher than the translational velocity. In the simplest variant of VR exchange theory [33], the dynamic parameters of VT and VV' exchange theory characterizing translational motion (reduced mass and velocity) are replaced with the corresponding parameters characterizing rotational motion (in this approximation, the role of translational motion is to bring the molecules closer). In view of this (for details, see [34, 35]), when calculating the rate constants of these exchange processes in terms of formulas (A.3)–(A.6), we used the relationship

$$\xi_0^{(m)} \approx \pi\beta\alpha^{-1}(D/kT)^{-1/2}$$

instead of formula (A.5) to obtain SSHM estimates in the calculation of the adiabaticity parameter $\xi_0^{(m)}$.

ACKNOWLEDGMENTS

This work was supported by the Russian Foundation for Basic Research, grant no. 040332678.

REFERENCES

1. Mallard, W.G., Westley, F., Herron, J.T., and Hampson, R.F., *NIST Chemical Kinetics Database, Version 6.0*, Gaithersburg, Md.: National Inst. of Standards and Technology, 1994.
2. Warnatz, J., in *Combustion in Chemistry*, Gardiner, W.C., Jr., Ed., New York: Springer, 1984, ch. 5.
3. Skrebkov, O.V. and Karkach, S.P., *Kinet. Katal.*, 2007, vol. 48, no. 3, p. 388 [*Kinet. Catal.* (Engl. Transl.), vol. 48, no. 3, p. 367].
4. Skrebkov, O.V. and Karkach, S.P., *Fiziko-khimicheskaya kinetika v gazovoi dinamike* (Physicochemical Kinetics in Gas Dynamics), 2004, vol. 2, http://wwwchemphys.edu.ru.
5. Popov, N.A., *Teplofiz. Vys. Temp.,* 2007, vol. 45, no. 2, p. 296 [*High Temp.* (Engl. Transl.), vol. 45, no. 2, p. 261].
6. Starik, A.M. and Titova, N.S., *Kinet. Katal.*, 2003, vol. 44, no. 1, p. 35 [*Kinet. Catal.* (Engl. Transl.), vol. 44, no. 1, p. 28].
7. Belles, F.E. and Lauver, M.R., *J. Chem. Phys.*, 1964, vol. 40, p. 415.
8. Vasil'ev, V.M., Kulikov, S.V., and Skrebkov, O.V., *Zh. Prikl. Mekh. Tekh. Fiz.*, 1977, vol. 4, no. 4, p. 13.
9. Skrebkov, O.V. and Kulikov, S.V., *Chem. Phys.*, 1998, vol. 227, p. 349.
10. Huber, K.-P. and Herzberg, G., *Molecular Spectra and Molecular Structure*, New York: Van Nostrand, 1979.
11. *NIST Standard Reference Data*, http:://webbook.nist.gov/chemistry/enthalpy.html.
12. Ryu, S.O., Hwang, S.M., and Rabinovitz, M.J., *J. Phys. Chem.*, 1995, vol. 99, p. 13984.
13. Michael, J.V., Sutherland, J.W., Harding, L.B., and Wagner, A.F., *Proc. Combust. Inst.*, 2000, vol. 28, p. 1471.
14. Fairchild, P.W., Smith, G.P., and Crosley, D.R., *J. Chem. Phys.*, 1983, vol. 79, p. 1795.
15. Smith, G.P. and Crosley, D.R., *J. Chem. Phys.*, 1986, vol. 85, p. 3896.
16. Carrington, T., *J. Chem. Phys.*, 1959, vol. 30, p. 1087.
17. Smekhov, G.D., Ibragimova, L.B., Karkach, S.P., Skrebkov, O.V., and Shatalov, O.P., *Teplofiz. Vys. Temp.*, 2007, vol. 45, no. 3, p. 440 [*High Temp.* (Engl. Transl.), vol. 45, no. 3, p. 395].
18. Wadlinger, R.L. and Darwent, B., deB, *J. Phys. Chem.*, 1967, vol. 71, p. 2057.
19. Stannard, P.R., Elert, M.L., and Gelbart, W.M., *J. Chem. Phys.,* 1981, vol. 74, p. 6050.
20. Sibert, E.L., Reinhardt, W.P., and Hynes, J.T., *J. Chem. Phys.*, 1982, vol. 77, p. 3583.
21. Sibert, E.L., Hynes, J.T., and Reinhardt, W.P., *J. Chem. Phys.*, 1982, vol. 77, p. 3595.
22. Dobbyn, A.J., Stumpf, M., Keller, H.-M., and Schinke, R., *J. Chem. Phys.*, 1996, vol. 104, p. 8357.

23. Mandelshtam, V.A., Taylor, H.S., and Miller, W.H., *J. Chem. Phys.*, 1996, vol. 105, p. 496.

24. Zhang, D.H. and Zhang, J.Z.H., *J. Chem. Phys.*, 1994, vol. 101, p. 3671.

25. Skrebkov, O.V., Karkach, S.P., Ivanova, A.N., Kostenko, S.S., *Fiziko-khimicheskaya kinetika v gazovoi dinamike* (Physicochemical Kinetics in Gas Dynamics), 2008, vol. 6, http://wwwchemphys.edu.ru.

26. Nikitin, E.E., Osipov, A.I., and Umanskii, S.Ya., in *Khimiya plazmy* (Plasma Chemistry), Smirnov, B.M., Ed., Moscow: Energoatomizdat, 1989, issue 15, p. 3.

27. Skrebkov, O.V. and Smirnov, A.L., *Khim. Fiz.*, 1991, vol. 10, no. 8, p. 1036.

28. Smirnov, A.L. and Skrebkov, O.V., *Khim. Fiz.*, 1992, vol. 11, no. 1, p. 35.

29. Skrebkov, O.V., Myagkov, Yu.P., Karkach, S.P., Vasil'ev, V.M., and Smirnov, A.L., *Dokl. Akad. Nauk*, 2002, vol. 383, no. 6, p. 1 [*Dokl. Phys. Chem.* (Engl. Transl.), vol. 383, nos. 4–6, p. 96].

30. Skrebkov, O.V., Karkach, S.P., and Smirnov, A.L., *Chem. Phys. Lett.*, 2003, vol. 375, p. 413.

31. Herzfeld, K.F. and Litovitz, T.A., *Absorption and Dispersion of Ultrasonic Waves*, New York: Academic, 1959.

32. Biryukov, A.S. and Gordiets, B.F., *Zh. Prikl. Mekh. Tekh. Fiz.*, 1972, no. 6, p. 29.

33. Moore, C.B., *J. Chem. Phys.,* 1965, vol. 43, p. 2979.

34. Ormonde, S., *Rev. Mod. Phys.*, 1975, vol. 47, no. 1, p. 193.

35. Eletskii, A.V., *Usp. Fiz. Nauk*, 1981, vol. 134, no. 2, p. 237.

36. Nikitin, E.E. and Osipov, A.I., *Itogi Nauki Tekh., Ser.: Kinet. Katal.*, 1977, vol. 4.

37. Basevich, V.Ya., Belyaev, A.A., and Posvyanskii, V.S., *Khim. Fiz.,* 1982, no. 6, p. 842.

38. Safaryan, M.N. and Skrebkov, O.V., *Fiz. Goreniya Vzryva*, 1975, no. 4, p. 614.

39. Volokhov, V.M. and Skrebkov, O.V., *Fiz. Goreniya Vzryva,* 1981, no. 4, p. 91.

40. Volokhov, V.M. and Skrebkov, O.V., *Khim. Fiz.*, 1984, vol. 3, no. 2, p. 224.

41. Skrebkov, O.V., *Zh. Prikl. Mekh. Tekh. Fiz.*, 1991, no. 6, p. 3.

42. Skrebkov, O.V., *Chem. Phys.*, 1995, vol. 191, p. 87.